A Multivariate Regression Model Between the October Rainfall Anomalies in Central America and the Tropical Pacific and Atlantic Ocean

Eric J. Alfaro
DFAOP-School of Physics and Geophysical Research Center, University of Costa Rica, San Jose, Costa Rica

Project Presented in the First Workshop on Regional Climate Prediction and Applications-Tropical Atlantic Basin, staged by Cooperative Institute for Mesoscale Meteorological Studies, The University of Oklahoma, Norman, Ok, USA

October 11- November 12, 1999
College of Continuing Education, The University of Oklahoma, Norman, Ok, USA

ABSTRACT

Principal Component Analysis was used to identify common anomaly patterns amongst 72 rainfall gauge stations in Central America during October, in order to identify stations to form October Rainfall Indices. October was chosen because it represents the center of the rainfall seasons, and previous studies have shown how ocean-atmosphere relations with Central American rainfall vary according to the rainfall month. Five rainfall regions where identified through this process, and the standardized rainfall anomaly time series was calculated for each region. A Multivariate Regression model was fitted to quantify the ocean-atmosphere interaction between the Tropical Pacific and Atlantic Ocean indices and each of the Rainfall indices. These models show that the Niño 4 region has the largest influence over the region when compared with the influence of the other candidate ocean indices, Niño 4 having negative correlation with all the Rainfall Indices. In addition, the Tropical North Atlantic index was found to have positive correlations with some of the Central America October rainfall regions. This work shows that the variability of the Tropical Eastern Pacific sea surface temperature anomaly (SSTA) presents stronger associations with the October Central America rainfall, than the Tropical North Atlantic SSTA. This is in contrast to stationary studies, which was previously shown to be more strongly associated with the Tropical North Atlantic SSTA. It is thought that the October result is mainly related to the Pacific SSTAs modifying the depth and degree of development of mesoscale convection.

Introduction

Most of the climatic variations and resulting impacts on human populations in Central America derive from the non-seasonal variations that accompany interannual and interdecadal changes in the Tropical Atlantic and Pacific Oceans and their interactions with the overlying troposphere. The intensity and duration of rainy season are important aspects of these interactions. These aspects affect agriculture, energy, hydrological resources and fishing (Waylen et al., 1996; Maul, 1993), but, the complex geography and the lack of good data sets, have made that relation difficult to quantify, yet clearly the Central America region has a strong climatic association, through teleconnection mechanisms, with the East Equatorial Pacific (El Niño region, mainly) and Tropical North Atlantic (Waylen et al., 1994). Also, the practical reasons mentioned above account for the lack of efforts on local climate prediction (Hastenrath, 1995).

For the Central America region, Alfaro and Cid (1999) used cluster analysis to identify common patterns of 72 precipitation gauge stations. With their anomaly time series as grouping variables, five clusters where identified through this process. A Vector Auto Regressive-Moving Average (VARMA) model was fitted to the data to quantify the ocean-atmosphere interaction between the oceanic indices of the Tropical North and South Atlantic, the Tropical Eastern Pacific and the first EOF's of the regional rainfall clusters. This model shows that the Tropical North Atlantic has the largest influence over the region when compared with the influence of the other indices, having positive correlation with all the rainfall EOF's. In addition, the Niño 3 index showed negative correlation with the rainfall clusters of the Pacific Slope, while the Tropical South Atlantic index, instead, was found to have no correlation with the annual rainfall of the region (though this may be different for individual months). Overall, that work showed that, using monthly rainfall data but supposing a stationary relationship, it is, the same relationship all aroud the year, the variability of the Tropical North Atlantic sea surface temperature anomaly (SSTA) presents stronger associations with the monthly precipitation of Central America rainfall, than the Tropical Eastern Pacific SSTA, mainly related to the degree of development of the Tropical Upper Tropospheric Trough (TUTT) descrived by Knaff (1997).

Additionally, Enfield and Alfaro (1999) and Alvarado (1999) had shown that the influence of the surrounding oceans is not stationary around the year. Thus, the main aims of this work are:

1) To quantify the influence of the Atlantic and Pacific inter-annual variability on Central America monthly rainfall anomalies. As a first month to start the analysis, October has been chosen, the peak of the rainy season.
2) To create an easy analysis framework that could be used in model construction for other months to forecast the monthly precipitation in the sub-regions of Central America.
3) To give physical significance to the statistical relationships, and therefore give confidence to the forecast systems.

Data and Study Area

Monthly data were used from 72 gauge stations, located in the Central America isthmus, from Guatemala and Belize in the North to Costa Rica and Panama in the South (Figs. 1-4) (see the details of the stations in Alfaro and Cid, 1999). The period of this study was from January 1960 to December 1995. To quantify the relationships of the precipitation with the atmospheric and oceanic fields, the following data were used:

a) Reanalysis Sea Level Pressure (SLP) and Wind (850 and 200 hPa levels) data.
b) Satellite Outgoing Long wave Radiation (OLR, from 01/74 to 12/97) data.
c) Sea Surface Temperature (SST) data.

Methodology

First, as a grouping procedure, the October rainfall mean standardized anomalies (base period, 1961-1990) were submitted to a rotated varimax principal component analysis (PCA). Plotting the PCA loadings, stations with common variance were grouped, and the rainfall indices were computed as the average of the grouped stations. Then, these rainfall indices were correlated with the October SST, SLP, Wind and OLR fields, to describe the physical relation between the variables. In order to identify a prediction relation, the correlations with the SST field were lagged from July to September. The oceanic regions that showed main prediction patterns were: (i) Niño 4 and (ii) the Tropical North Atlantic (NATL, 22°-2° N, 80°-15° W). The forecast models using these predictors are presented in the next section.

The criteria for the model construction were:

a) The Multiple $R \geq 0.4$.
b) The predictor coefficients' p_values ≤ 0.05 and tolerances ≥ 0.90.
c) A model F-ratio p_value ≤ 0.05.

Finally, the models were cross-validated for the same period of analysis and model verification included a categorical analysis of the forecast versus observed in the form of contingency tables.

Results

The grouping procedure identified 5 groups of stations in the region and they are plotted in Figs. 1-4, and described in table 1. The identification of this number of groups was based on the step of the eigen value plot. This analysis is entirely consistent with the cluster analysis presented in Alfaro and Cid (1999).

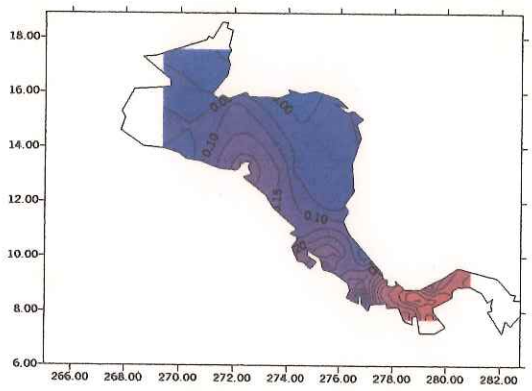

Fig. 1. Loadings of the first October rotated principal component (red => positives, blue => negatives, % of the total variance explained = 14.7).

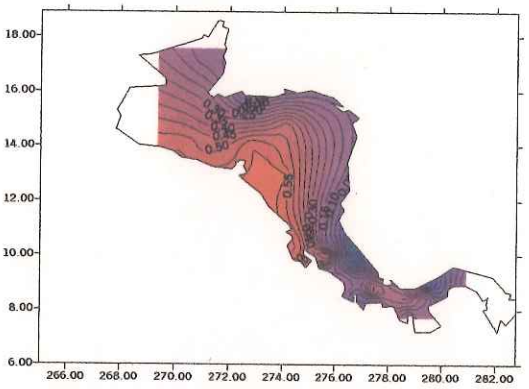

Fig. 2. Loadings of the second rotated principal component (red => positives, blue => negatives, % of the total variance explained = 9.9).

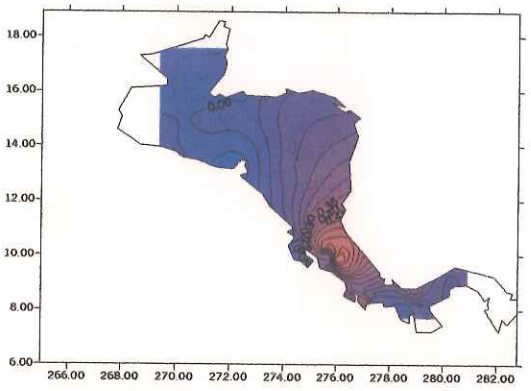

Fig. 3. Loadings of the third rotated principal component (red => positives, blue => negatives% of the total variance explained = 9.6).

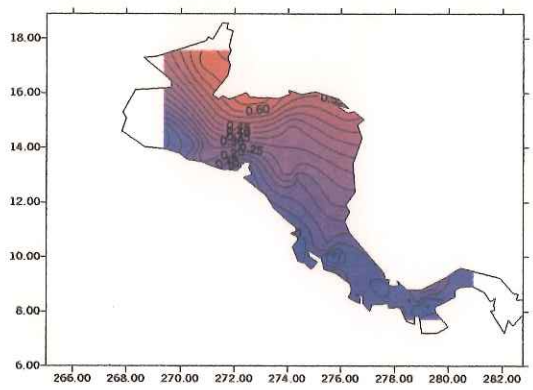

Fig. 4. Loadings of the fourth rotated principal component (red => positives, blue => negatives% of the total variance explained = 5.7).

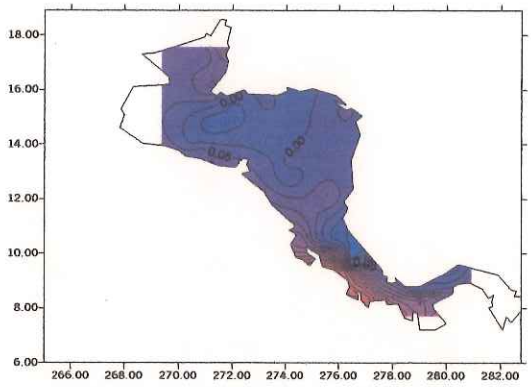

Fig. 5. Loadings of the fifth rotated principal component (red => positives, blue => negatives% of the total variance explained = 7.3).

Number of Index	Description	Number of Stations
1	Panama	24
2	North Pacific Slope (lat > 10°)	18
3	Costa Rica's Caribbean Slope	11
4	Honduras and Belize's Caribbean Coast	9
5	Costa Rican Central and South Pacific Coast	9

Table 1. Description of the October precipitation indices used in the analysis.

a) Index 1

The Fig. 6 shows a robust negative correlation with the SST fields in the Tropical Pacific, chich actually extends into the Caribbean basin. Though the correlation SLP values are low (Fig. 7), there is a weak zonal pattern, with positive values in the West and negatives values in the East of Panama, that is consistent with the weak negative OLR correlation values over Panama (Fig. 8) and also with the West wind component correlation at low

levels (Fig. 9).The winds at 200 hPa show a well defined cyclonic circulation over the Caribbean.

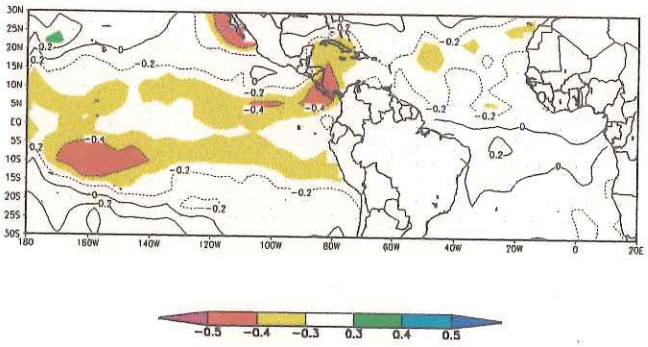

Fig. 6. October SST vs. Index 1 correlations.

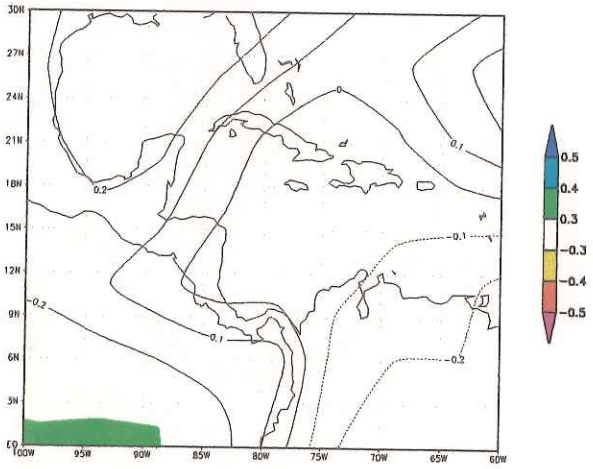

Fig. 7. October SLP vs. Index 1 correlations.

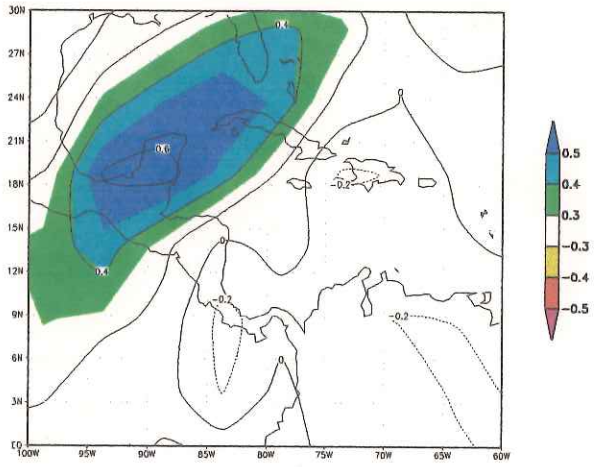

Fig. 8. October OLR vs. Index 1 correlations.

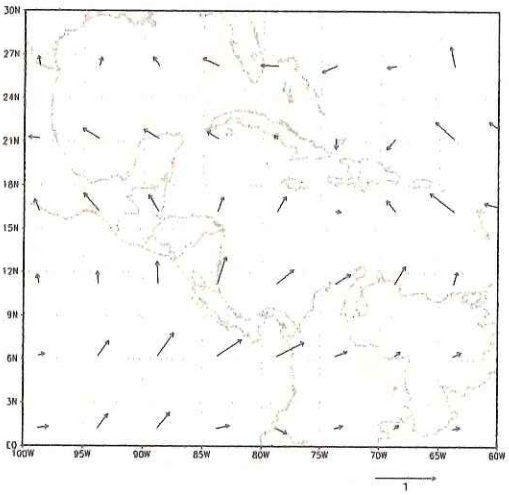

Fig. 9. October 850 hPa Wind vs. Index 1 correlations.

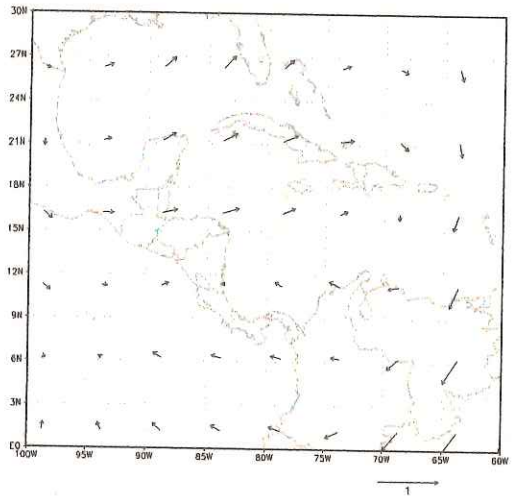

Fig. 10. October 200 hPa Wind vs. Index 1 correlations.

The forecast model fitted was:

Effect	Coefficient	p_value
CONSTANT	-0.031	0.758
Niño4_7	-0.512	0.011

Multiple R: 0.42, F-ratio: 7.286, p_value: 0.011

Where Niño4_7 indicates July values of the Niño4 SSTA.

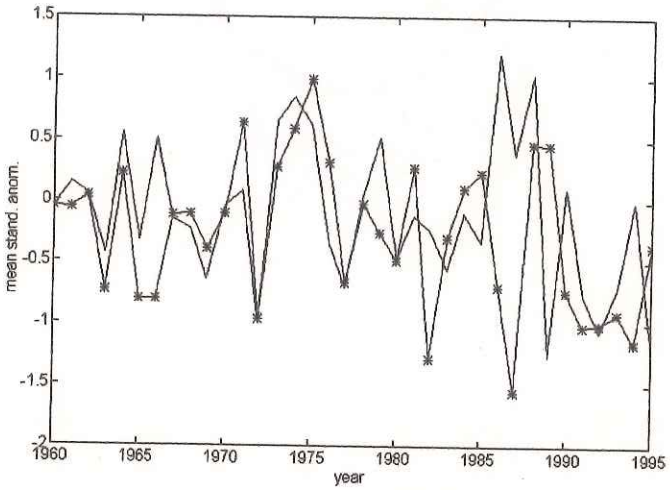

Fig. 11. Observed (continuous line) and cross-validated estimated (line with asterisks) values for the Index 1, Skill = 0.301.

Obs\Est	BN	N	AN	Total
BN	5	5	2	12
N	3	5	4	12
AN	4	2	6	12
Total	12	12	12	36

Test statistic	Value	df	Prob.
Pearson Chi-square	4.000	4.000	0.406

Table 2. Contingency table for the predicted Index 1 values. Hit Rate = 44.4%, Hit Skill = 16.7%, LEPS Skill = 19.5%, FAR(BN) = 33%, FAR(AN) = 17%, POD(BN) = 42%, POD(AN) = 50%.

b) Index 2

Fig. 12 shows the correlation between the SST field and the Index 2. There is a noticeable pattern of negative values in almost all the Equatorial Pacific Ocean and positive values in the Gulf of Mexico. The correlation map with the SLP (Fig. 13) show negative values that are consistent with the negative ones in the OLR field (Fig. 14) and with the West component relationship with the wind in low level (Fig. 15). The winds in 200 hPa, show a well defined Northeasterly correlation pattern (Fig. 16).

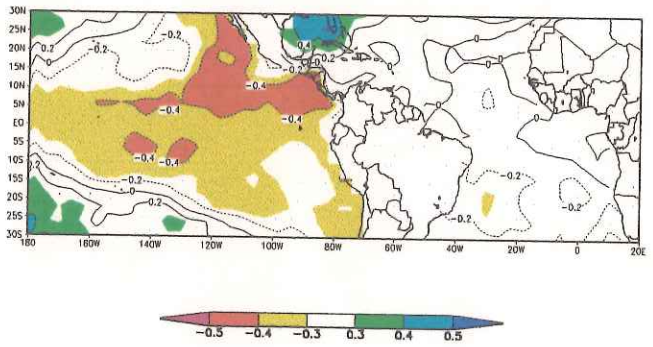

Fig. 12. October SST vs. Index 2 correlations.

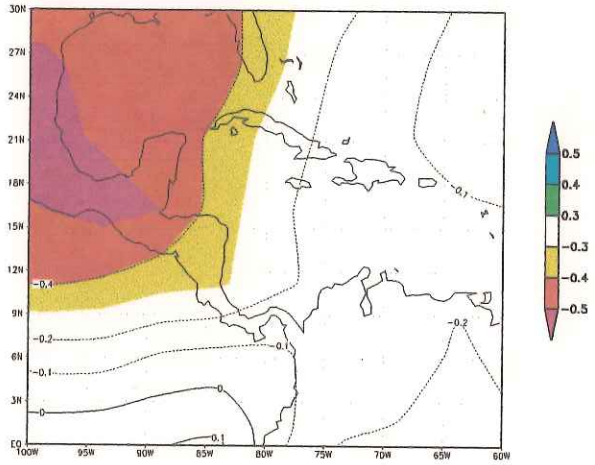

Fig. 13. October SLP vs. Index 2 correlations.

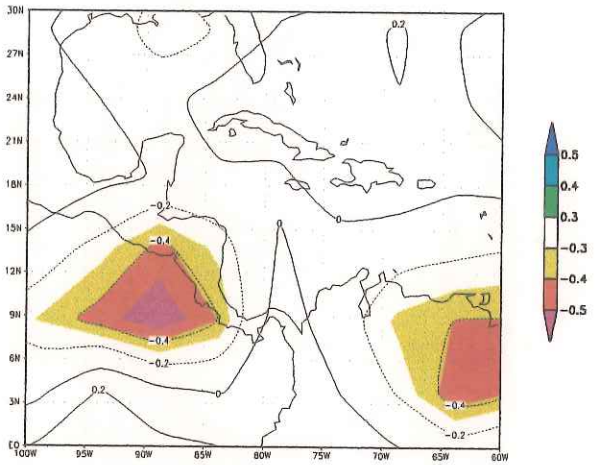

Fig. 14. October OLR vs. Index 2 correlations.

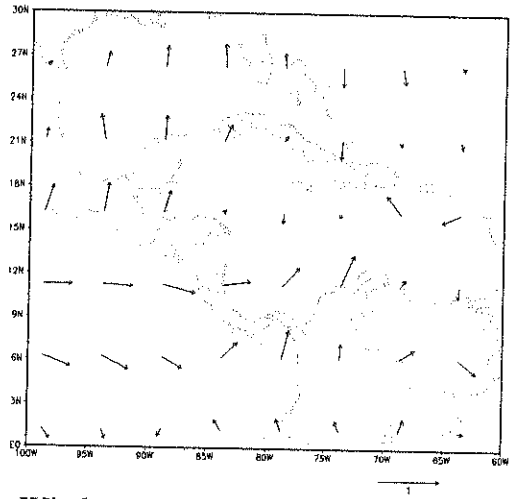

Fig. 15. October 850 hPa Wind vs. Index 2 correlations.

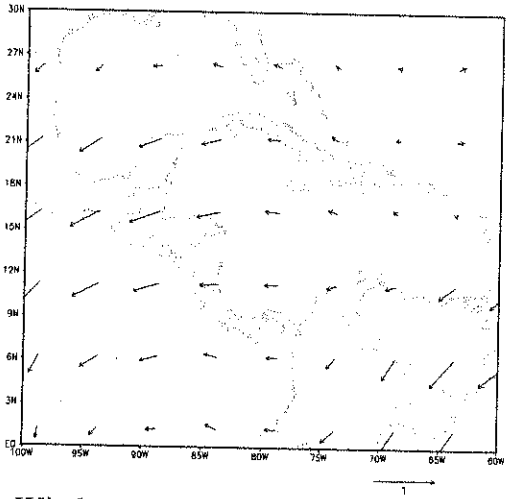

Fig. 16. October 200 hPa Wind vs. Index 2 correlations.

The model fitteded was:

Effect	Coefficient	p_value
CONSTANT	4.343	0.024
NATL7	0.859	0.027
Niño4_7	-0.547	0.008

Multiple R: 0.52, F-ratio: 6.233, p_value: 0.005

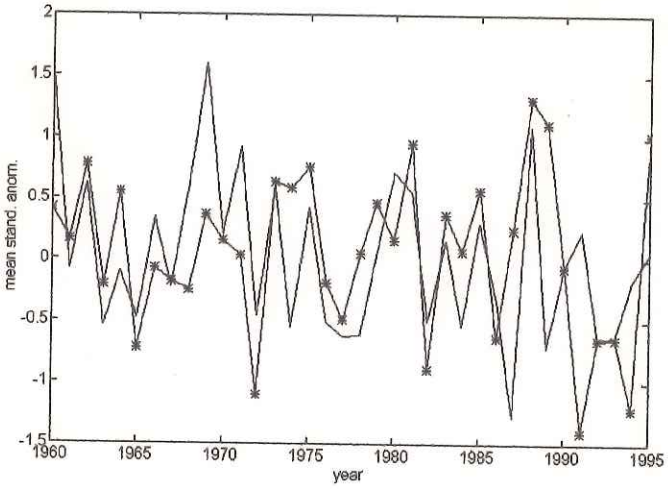

Fig. 17. Observed (continuous line) and estimated (line with asterisks) values for the Index 2, Skill = 0.376.

Obs\Est	BN	N	AN	Total
BN	7	3	2	12
N	4	5	3	12
AN	1	4	7	12
Total	12	12	12	36

Test statistic	Value	Df	Prob
Pearson Chi-square	8.500	4.000	0.075

Table 3. Contingency table for the predicted Index 2 values. Hit Rate = 52.8%, Hit Skill = 29.2%, LEPS Skill = 40.8%, FAR(BN) = 8%, FAR(AN) = 17%, POD(BN) = 58%, POD(AN) = 58%.

c) Index 3

The Fig. 18 shows the global SST correlation with the Index 3. There is a noticeable negative correlation pattern with the Niño 4 region (but weaker than previous indices) and an area located in the North Eastern Tropical Pacific (~ 10N, 100W). TheSST anomalies in this region could be created by the wind anomalies associated also with the rainfall anomalies, e.g. the response of the atmopshere, forced by the Nino3/4 region. The Figs. 19 and 21 show an inconsistent pattern in the pressure and winds that could be caused by the resolution of the data. The Fig. 20 shows a negative correlation pattern over almost all the South part of the region and the Fig. 22 shows a very cyclonic circulation at 200hPa in almost all the Caribbean region.

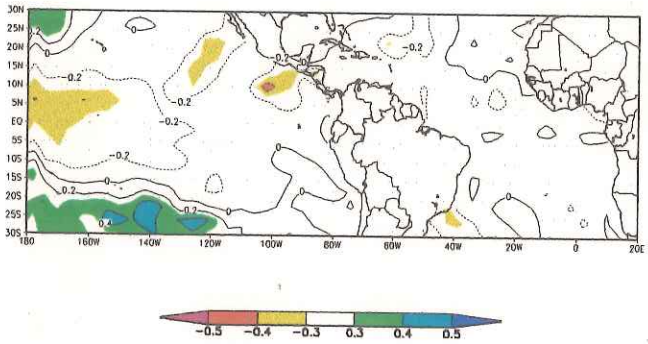

Fig. 18. October SST vs. Index 3 correlations.

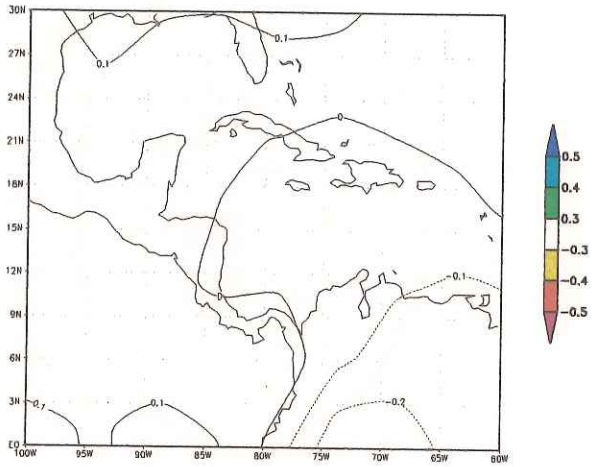

Fig. 19. October SLP vs. Index 3 correlations.

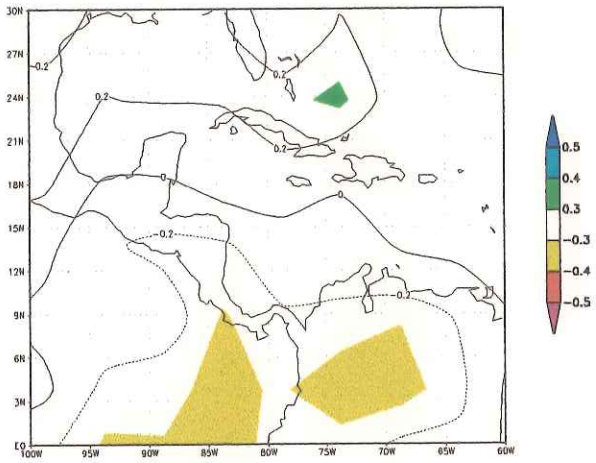

Fig. 20. October OLR vs. Index 3 correlations.

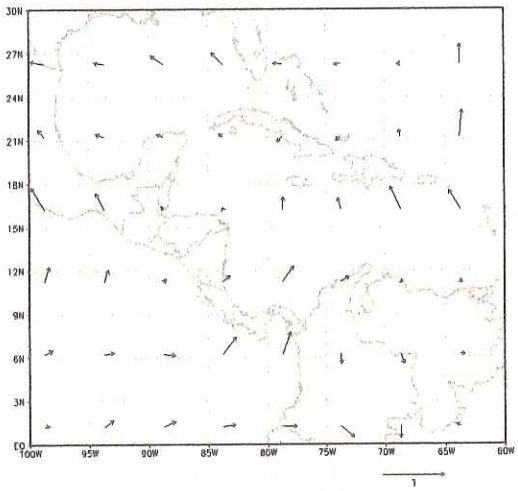

Fig. 21. October 850 hPa Wind vs. Index 3 correlations.

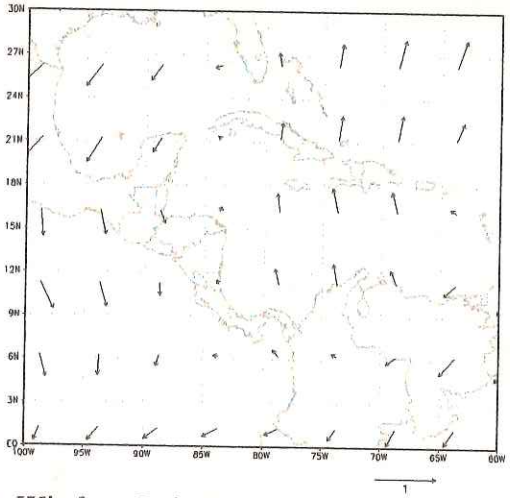

Fig. 22. October 200 hPa Wind vs. Index 3 correlations.

The model fitted was:

Effect	Coefficient	p_value
CONSTANT	4.121	0.030
NATL7	0.831	0.031
Niño4_9	-0.377	0.024

Multiple R: 0.49, F-ratio: 5.209, p_value: 0.011

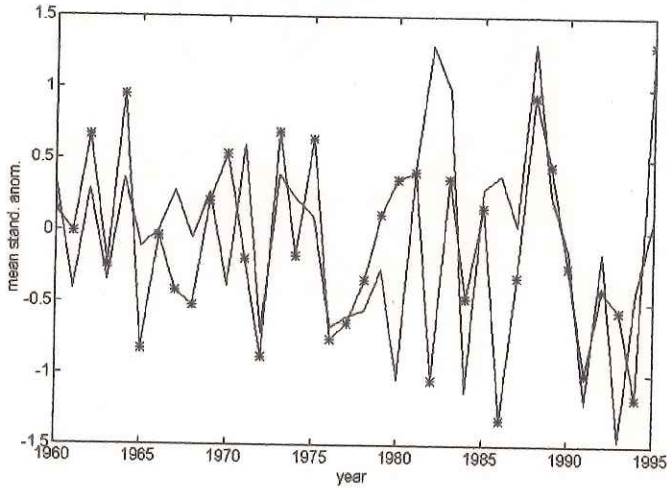

Fig. 23. Observed (continuous line) and estimated (line with asterisks) values for the Index 3, Skill = 0.359.

Obs\Est	BN	N	AN	Total
BN	7	2	3	12
N	3	6	3	12
AN	2	4	6	12
Total	12	12	12	36

Test statistic	Value	Df	Prob
Pearson Chi-square	7.000	4.000	0.136

Table 4. Contingency table for the predicted Index 3 values. Hit Rate = 52.8%, Hit Skill = 29.2%, LEPS Skill = 32.0%, FAR(BN) = 25%, FAR(AN) = 17%, POD(BN) = 58%, POD(AN) = 50%.

d) Index 4

This index shows a well-defined negative correlation pattern with the Niño 4 region (Fig. 24), but there was not found any significant relationship in the SLP field (Fig. 25). Index 4 also shows correlation in the Equatorial/South Atlantic SST – but it was not useful for the prediction model because there was not found any strong lag correlation. The OLR (Fig. 26) shows a very distinctive pattern with strong negative correlations over the rainfall index region (which is physically what we expect) and it is consistent with the 850-hPa wind correlations that show an "easterly wave" pattern. The winds at the 200-hPa levels show a noticeable northerly component over the area of the rainfall index.

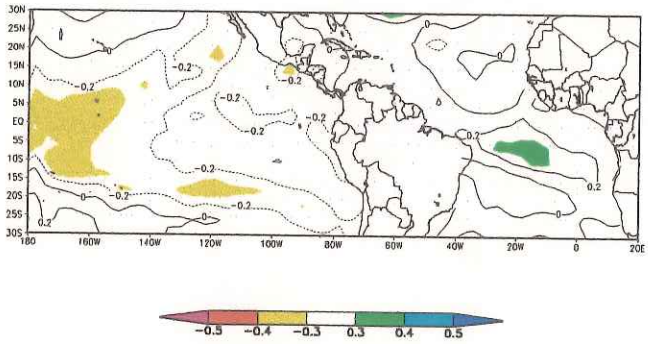

Fig. 24. October SST vs. Index 4 correlations.

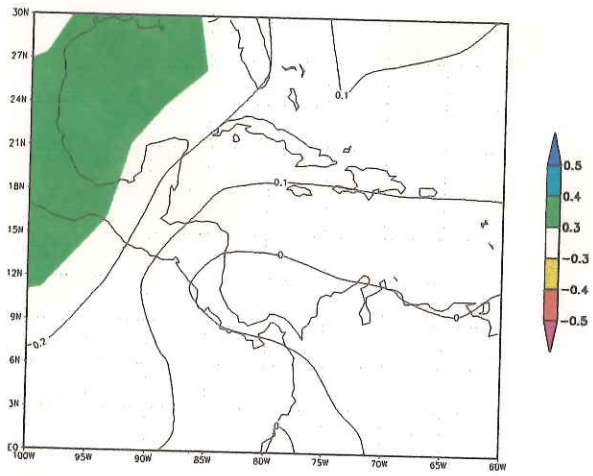

Fig. 25. October SLP vs. Index 4 correlations.

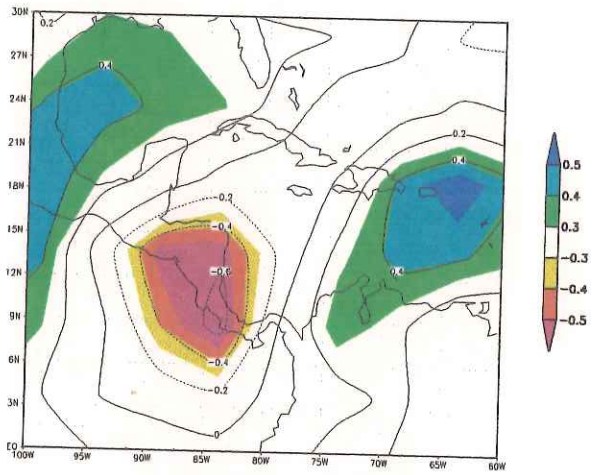

Fig. 26. October OLR vs. Index 4 correlations.

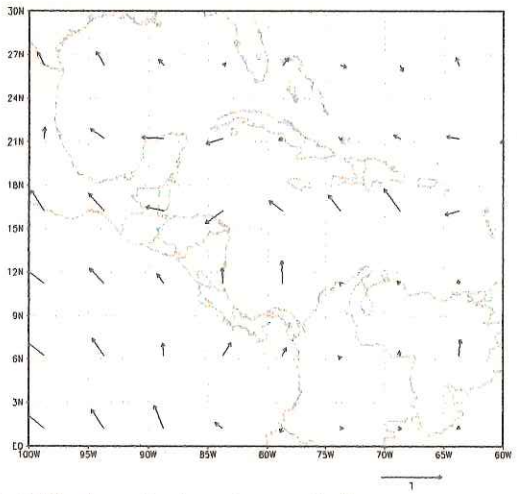

Fig. 27. October 850 hPa Wind vs. Index 4 correlations.

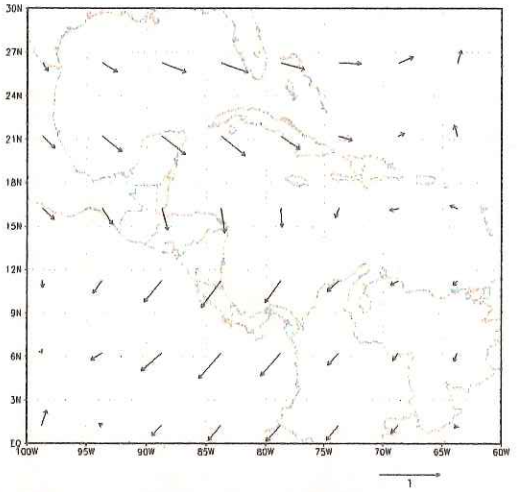

Fig. 28. October 200 hPa Wind vs. Index 4 correlations.

The model fitted was:

Effect	Coefficient	p_value
CONSTANT	0.035	0.731
Niño4_8	-0.480	0.016

Multiple R: 0.40, F-ratio: 6.452, p_value: 0.016

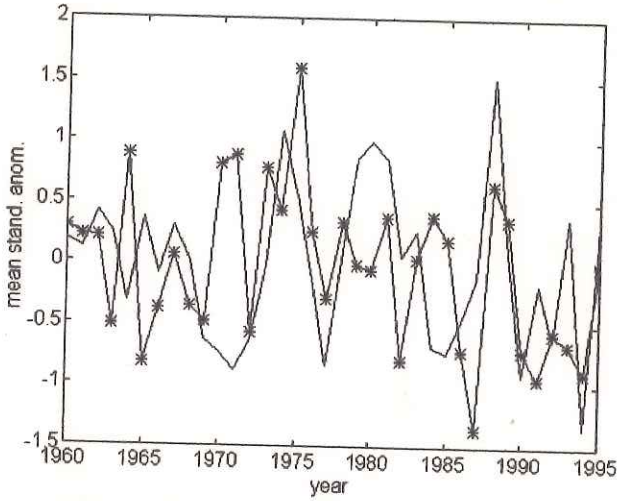

Fig. 29. Observed (continuous line) and estimated (line with asterisks) values for the Index 4, Skill = 0.345.

Obs\Est	BN	N	AN	Total
BN	6	2	4	12
N	4	4	4	12
AN	2	6	4	12
Total	12	12	12	36

Test statistic	Value	df	Prob
Pearson Chi-square	4.000	4.000	0.406

Table 5. Contingency table for the predicted Index 4 values. Hit Rate = 38.9%, Hit Skill = 8.3%, LEPS Skill = 14.1%, FAR(BN) = 17%, FAR(AN) = 33%, POD(BN) = 50%, POD(AN) = 33%.

e) Index 5

In the Fig. 30 are shown the correlations between the Index 5, there is a remarkable negative pattern that extends from the date line to Central America. As with the rainfall Index 1, this index shows a relationship with a weak but clear SLP gradient across the isthmus with relative high pressures in the West and relative low pressure in the East (Fig. 31), this is consistent with: a) the negative correlation with the OLR (Fig. 32) and b) the Southwest component in the wind in the 850 hPa (Fig. 33). The wind correlation at the 200-hPa level shows an Eastward direction over the region (Fig. 34).

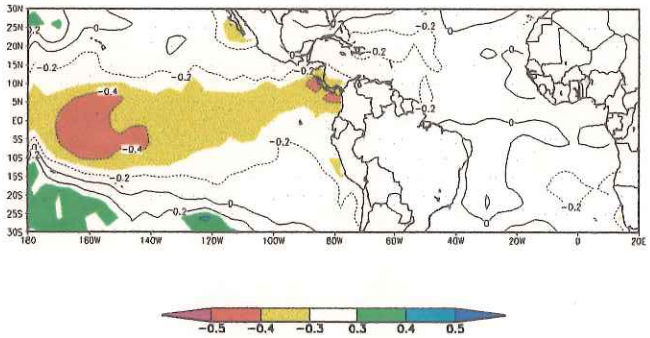

Fig. 30. October SST vs. Index 5 correlations.

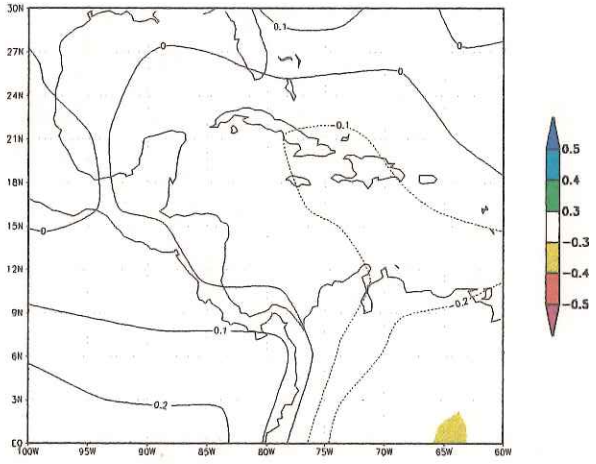

Fig. 31. October SLP vs. Index 5 correlations.

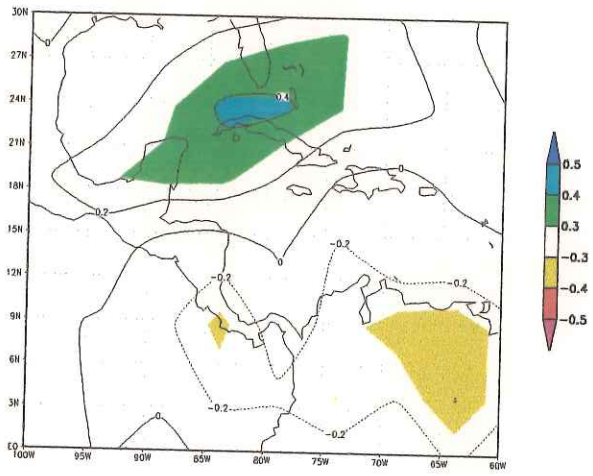

Fig. 32. October OLR vs. Index 5 correlations.

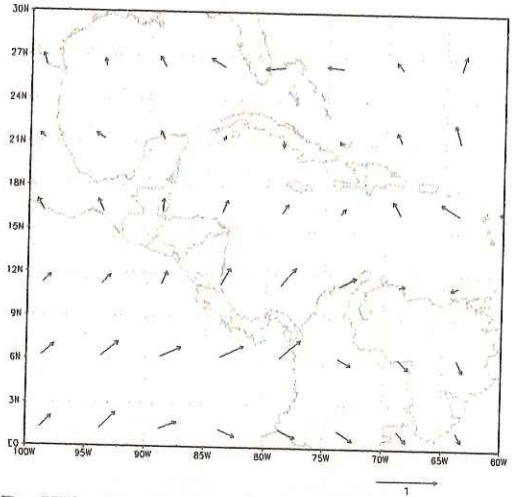

Fig. 33. October 850 hPa Wind vs. Index 5 correlations.

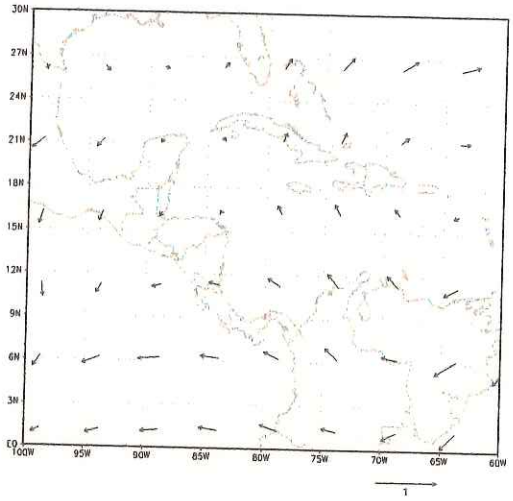

Fig. 34. October 200 hPa Wind vs. Index 5 correlations.

The model fitted was:

Effect	Coefficient	p_value
CONSTANT	0.071	0.577
Niño4_7	-0.684	0.008

Multiple R: 0.43, F-ratio: 7.837, p_value: 0.008

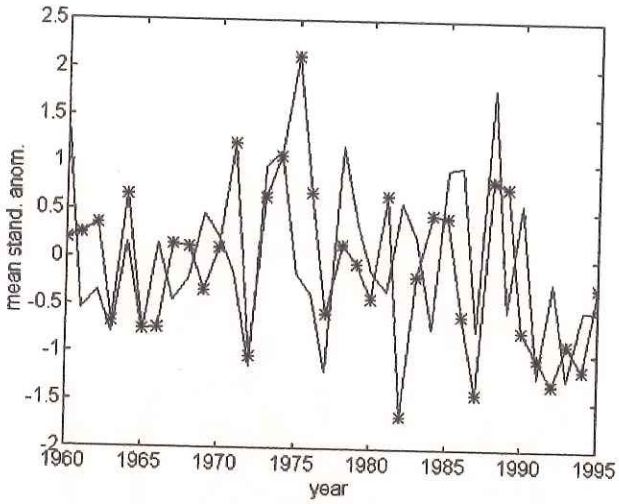

Fig. 35. Observed (continuous line) and estimated (line with asterisks) values for the Index 5, Skill = 0.316.

Obs\Est	BN	N	AN	Total
BN	7	3	2	12
N	2	4	6	12
AN	3	5	4	12
Total	12	12	12	36

Test statistic	Value	df	Prob
Pearson Chi-square	6.000	4.000	0.199

Table 6. Contingency table for the predicted Index 5 values. Hit Rate = 41.7%, Hit Skill = 12.5%, LEPS Skill = 21.2%, FAR(BN) = 25%, FAR(AN) = 17%, POD(BN) = 58%, POD(AN) = 33%.

Discussion and Conclusions

As in Alfaro and Cid (1999), the present study shows that two oceanic regions, the Tropical Pacific and Atlantic, clearly influence the rainfall anomaly fields of Central America. These relationships are persistent in time and permit the construction of prediction models based on lag oceanic schemes, here from two to zero month lead time (July to September) using the Multivariate Correlation. The variability in the month of absolute maximum correlation is in part due to sampling error. The method here captures

just the lag month of absolute maximum correlation, but it was found for all predictors used here, that the same sign in the correlation persisted through all the four months July through October. Coupled with the consistent results with the SST correlation maps and the analyses with atmospheric data, there is little doubt that the models constructed here are rooted in the physics of the climate system and can be expected to have skill levels above the chance level when applied in real time. It was found that for October rainfall, the main influence on the region is the Niño 4 region with negative correlations (as described in Ropelewski and Halpert, 1987; 1989), and not the Tropical North Atlantic positive correlations (as in Alfaro and Cid, 1999). This appears to be a specific property of October rainfall. As is discussed in Enfield and Alfaro (1999) and Alvarado (1999), these relationships are not stationary around the year. The Figs. 11, 17, 23, 29 and 35 show that the forecast models for October are not useful to provide exact rainfall quantity predictions, because of their relatively low skills (correlations of 0.301-0.376), but the Tables 2-6 show that the models can be useful for categorical predictions (terciles), most especially for the extreme terciles (notice also that always skill is above the chance level, e.g. LEPS skills always > 0).

The rainfall Index correlations with the low level 850 hPa wind fields agree with previous studies on the region (e.g. Zarate, 1977), that links enhanced westerly component of the wind to positive rainfall anomalies in the Pacific Slope (Indices 1, 2 and 5), because it helps the depth of mesoscale convection over the region. The rainfall anomalies in the Caribbean Slope (Index 4) are more related to Atlantic disturbances like easterly waves. Despite many physically consistent signals emerging from the reanalysis and OLR datasets, it has also been noted that there were some inconsistencies in some of the atmospheric correlation fields. These might be explained by the grid resolution of the data that could obscure or distort some of the patterns.

As further work, it is recommended to create these kind of models for all the months (here the models are constructed to forecast October rainfall). The results of such an extended analysis could be summarized in a report that could be used and further developed by the Costa Rican Meteorological Institute (IMN) in a regional operational climate prediction network.

References

Alfaro, E. and L. Cid, 1999: Ajuste de un modelo VARMA para los campos de anomalías de precipitación en Centroamérica y los índices de los océanos Pacífico y Atlántico Tropical. *Atmósfera*, **12**(4), 205-222.

Alvarado, 1999: Alteración de la atmósfera libre sobre Costa Rica durante eventos de El Niño. Degree Thesis. School of Physics, University of Costa Rica, San José, Costa Rica.

Enfield, D. and E. Alfaro, 1999: The dependence of Caribbean rainfall on the interaction of the tropical Atlantic and Pacific Oceans. *J. Climate*, **12**, 2093-2103.

Hastenrath, S., 1995: Recent advances in the tropical climate prediction. *J. Climate*, **8**, 1519-1532.

Knaff, J., 1997: Implications of summertime sea level pressure anomalies in the Tropical Atlantic region. *J. Climate*, **10**, 789-804.

Maul, G., 1993: Implications of future climate on ecosystems and socio-economic structure in the marine and coastal regions of the Intra-Americas Sea. *Climatic Change in the Intra-Americas Sea*, G. Maul, Ed., Edward Arnold, 3-28.

Ropelewski, C., and M. Halpert, 1987: Global and regional scale precipitation associated with El Nino/Southern Oscillation. *Mon. Weather Rev*, **115**, 1606-1626.

Ropelewski, C., and M. Halpert, 1989: Precipitation patterns associated with the high index phase of the Southern Oscillation. *J. Climate*, 2, 268-284.

Waylen, P., C. Caviedes and M. Quesada, 1996: Interannual variability of monthly precipitation in Costa Rica. *J. Climate*, **9**, 2606-2613.

Waylen, P., M. Quesada and C. Caviedes, 1994: The effects of El Niño-Southern Oscillation on precipitation in San Jose, Costa Rica. *Int. J. Climatol.*, **14**, 559-568.

Zárate, E., 1977: Principales sistemas de vientos que afectan a Costa Rica y sus relaciones con la precipitación. Degree Thesis, School of Physics, University of Costa Rica, San José, Costa Rica, 61 pp.